Viscosity of $\{x\mathrm{CO_2} + (1\text{-}x)\mathrm{CH_4}\}$ with $x = 0.5174$ for Temperatures Between (229 and 348) K and Pressures Between (1 and 32) MPa.

Clayton R. Locke, Paul L. Stanwix, Thomas J. Hughes, Michael L. Johns, Anthony R. H. Goodwin[†,a]*, Kenneth N. Marsh, Guillaume Galliero*[††]*, Eric F. May*[b].

Centre for Energy, School of Mechanical & Chemical Engineering, The University of Western Australia, Crawley, WA, 6009, Australia

[†]also Schlumberger Technology Corporation, Sugar Land, Texas 77478, United States

[††]Laboratoire des Fluides Complexes et leur Réservoirs, (UMR-5150 with CNRS and TOTAL), Université de Pau et des Pays de l'Adour, BP 1155, 64013 PAU Cedex, France

Abstract

A vibrating wire instrument, in which the wire was clamped at both ends, was used to measure the viscosity of $\{x\mathrm{CO_2} + (1\text{-}x)\mathrm{CH_4}\}$ with $x = 0.5174$ with a combined uncertainty of 0.24 μPa·s (a relative uncertainty of about 0.8 %) at temperatures T between (229 and 348) K and pressures p from (1 to 32) MPa. The corresponding mass density ρ, estimated with the GERG-2008 equation of state, varied from (20 to 600) kg·m^{-3}. The measured viscosities were consistent

---

[a] Deceased.

[b] Corresponding author. Tel: +61 8 6488 2954 Fax.: +61 8 6488 1024. *E-mail address:* eric.may@uwa.edu.au

within combined uncertainties with data obtained previously for this system using entirely different experimental techniques. The new data were compared with three corresponding states-type models frequently used for predicting mixture viscosities: the extended corresponding states (ECS) model implemented in REFPROP 9.1; the SUPERTRAPP model implemented in MultiFlash 4.4; and a corresponding states model derived from molecular dynamics simulations of Lennard Jones fluids. The measured viscosities deviated systematically from the predictions of both the ECS and SUPERTRAPP models with a maximum relative deviations of 11 % at (229 K, 600 kg·m^{-3}) and -16 % at (258 K, 470 kg·m^{-3}), respectively. In contrast, the molecular dynamics based corresponding states model, which is predictive for mixtures in that it does not contain any binary interaction parameters, reproduced the density and temperature dependence of the measured viscosities well, with relative deviations of less than 4.2 %.

Keywords: Viscosity; Carbon dioxide: Methane; Density; Molecular Dynamics, Corresponding States.

1. Introduction

Carbon dioxide is ubiquitous in natural gas; according to the International Energy Agency, about 43 % of the world’s natural gas reserves, excluding North America, contain significant amounts of acidic gases such as H_2S and CO_2 [1]. Determinations of the thermophysical properties of gaseous mixtures of hydrocarbons with CO_2 are required for optimal exploitation and usage in industry. One specific example where the viscosity of CO_2 + CH_4 mixtures is relevant is Enhanced Gas Recovery (EGR) [2,3], which is a prospective technology whereby CO_2 is injected into natural gas reservoirs to sustain pressure and hence increase natural gas production; it also thus provides an economically-incentivised means of CO_2 sequestration.

These supercritical fluids are, however, completely miscible and thus reservoir simulations of EGR processes are required to assess their viability for a given field scenario. One of the required inputs into these simulations is the dependence of viscosity on the $CO_2 + CH_4$ mixture composition, temperature and pressure. A second example is in the cryogenic processing of natural gas: more accurate predictions of gas mixture viscosities at low temperatures and high pressures would help improve simulations of the Controlled Freeze Zone [4] process or the Rectisol process [5,6], which are intended to achieve CO_2 content specifications for pipeline gas and LNG, respectively.

Methods for predicting viscosity have been reviewed by, for example, Vesovic [7] where the Lohrentz-Bray-Clark, Pedersen, SUPERTRAPP, and Vesovic-Wakeham models were evaluated against (limited) available experimental data. Experimental determinations of viscosity for $\{xCO_2 + (1-x)CH_4\}$ with $x \approx 0.5$ in the pressure range (1 to 35) MPa are limited in the archival literature to those of the authors' previous measurements at moderate densities [8], the measurements of De Witt and Thodos [9], and those of Kestin et al. [10,11], both from the 1960's. (We note the existence of literature data from 1956 of Jackson [12], but have not included this data in our comparisons as they are limited to viscosities of $\{xCO_2 + (1-x)CH_4\}$ measured at room temperature and pressure, and are not particularly relevant to the range of pressures and temperatures of this work.) Recently Davani et al.[13], using an oscillating piston viscometer, determined the viscosity of $\{xCO_2 + (1-x)CH_4\}$ with $x = 0.1$ at pressures from (35 to 170) MPa.

In this article, we report new measurements of the viscosity of $\{xCO_2 + (1-x)CH_4\}$ with $x = 0.5174$ at temperatures T between (229 to 348) K and pressures p between (1 to 32) MPa, which correspond to mass densities ρ of (20 to 600) $kg \cdot m^{-3}$. The viscosity η was measured with a vibrating-wire-viscometer (VWV), clamped at both ends and operated in steady-state mode that has been described in detail previously [8,14]. To calculate viscosity from the measured resonance curve, the fluid mass density is required and in this work it was calculated from the measured *T* and *p* using the GERG-2008 equation of state (EOS) [15] as implemented in the software package REFPROP (REFerence fluid PROPerties database 23, version 9.1, NIST) [16].

The measured viscosities were then compared with predictions made using one of three models based on the principle of corresponding states: the Extended Corresponding States (ECS) model implemented in REFPROP, the SUPERTRAPP model implemented in MultiFlash 4.4 [17,18] and a correlation based on molecular dynamics (MD) of Lennard Jones molecules that is predictive for mixtures [19]. This modified corresponding states approach has been further adapted to include molecules such as CO_2 and to deal with acid gas mixtures [20].

2. Experimental

The system and operating equations have been described in detail elsewhere [8], so only a brief description will be provided here. The wire was formed from a centerless ground tungsten rod (≈ 40 mm long, 50.8 μm diameter, mass fraction purity of 0.9995) clamped and held in tension by a wire holder assembly (formed from stainless steel and polyimide) to produce a vacuum mechanical resonance of about 2 kHz. The resonance frequency, which varied as a function of temperature because the linear thermal expansion of the wire material differed from that of the materials used to form the spacer, was selected so that the tension on the wire remained below 80 % of the yield strength of the wire. In the presence of a static magnetic flux (0.45 T), an alternating drive current excited the mechanical resonance of the wire. The amplitude of the drive signal applied to the wire was modified in accordance with the changing density to ensure that the maximum relative displacement was less than 1 % of the wire radius.

The amplitude of the wire's motion was monitored by observing the electromagnetically induced voltage, through demodulation using a lock-in amplifier; when the drive was at the mechanical resonance there was an amplification in the amplitude of vibration by the quality factor *Q*. Stepping the drive signal frequency *f* through resonance allowed the fluid viscosity to be determined by fitting the measured resonance to the two quadratures *u*(*f*) and *v*(*f*) of the hydrodynamic response function $\mathrm{V}_{\mathrm{hydro}}$ [21,22],

$$V_{\mathrm{hydro}}\left(f\right)=u\left(f\right)-\mathrm{i}v\left(f\right)=\frac{\left(A_1+\mathrm{i}A_2\right)f}{\mathrm{i}\left[f^2\left(1+\beta\right)-f_0^2\right]+f^2\left(\beta'+2\Delta_0\right)} \quad , \tag{1}$$

where A_1 and A_2 are amplitudes of the complex response, β is the dimensionless added mass of the fluid surrounding the wire, β' is the dimensionless viscous damping of the fluid surrounding the wire, and f_0 is the resonance frequency in vacuum. In equation 1, Δ_0 is the logarithmic decrement in vacuum (vacuum damping) characterizing all losses including those of the wire itself and the supporting structure, and for this apparatus was determined by measurements in vacuum to be $(2.148 \pm 0.012)\cdot 10^{-5}$. In principle, the method provides for an absolute measurement of viscosity, owing to the ability to determine all parameters of the measurement by independent means. Such a measurement has been done with water [23]. In most cases, however, the difficulty in determining the radius of thin wires with sufficient accuracy results in the requirement for calibration with a fluid of known density and viscosity. The radius of the wire used in this work was determined by calibration with helium for which the viscosity was determined from ab initio calculations combined with corresponding states [8].

The wire radius was chosen to satisfy the following competing criteria [24]; the radius *R* must be small enough in comparison with the length of the wire *L* (of order $R/L = 0.001$), but it must also be large enough to give a quality factor larger than ≈10. The wire used had a length L = 40 mm and a radius $\langle R\rangle = (25.518 \pm 0.065)$ μm, giving R/L = 0.0006 that permitted the measurement of viscosities up to about 500 μPa·s.

The operational parameters of the apparatus are summarized by Table 1 which lists the Type B uncertainty [25] contributions to the viscosity measurements. Previously [8], the VWV was used to measure the viscosity of a binary mixture $\{x\mathrm{CO_2} + (1-x)\mathrm{CH_4}\}$ with $x = 0.57 \pm 0.01$ (the composition in ref [8] was determined by gas chromatography) at densities up to 100 kg·m^{-3}. The results presented in this work used the same instrument to extend upon these measurements, this time with $x = 0.5174 \pm 0.0001$ (prepared gravimetrically, with methane and carbon dioxide of purity and sources listed in Table 2) at densities up to 600 kg·m^{-3}.

Table 1. Contribution to Type B uncertainty of the viscosities, $u_j(\eta)$, measured in this work.

source	$100 \cdot u_j(\eta)/\eta$
wire radius calibration	0.51
nonlinear motion/out of plane motion	0.44
density of wire material	0.09
mixture composition	0.02
vacuum damping	0.02
pressure sensor	0.005
temperature sensor	0.002
total	0.68

Table 2. Chemical sample sources. Purity was assumed and no further chemical analysis or purification was performed.

chemical name	source	manufacturer's purity in mole fraction
carbon dioxide	Coregas	0.99999
methane	BOC	0.99995

The relative uncertainty in the mole fraction was determined from the relative contributions arising from the measurement of mass (0.023 %), mole fraction purity of the component gases (0.005 %), and dead volume (0.003 %) in the cylinder valve. The uncertainty in the mole fraction corresponds to an uncertainty in the calculated viscosity of 0.005 μPa·s (a relative uncertainty of 0.02 %).

3. Results and discussion

The viscosity of $\{x\mathrm{CO_2} + (1-x)\mathrm{CH_4}\}$ with $x = 0.5174 \pm 0.0001$ listed in Table 3 was determined at each T and p from an average of between 5 and 7 up-down frequency-sweep pairs. Each sweep direction required $t \approx 40$ min, for a maximum measurement time per reported point of 4.7 h. Table 3 also lists the Type A uncertainties [25] of the measured viscosity that were determined from the standard deviation of up to 7 measurements, and the combined standard uncertainty at a coverage factor of $k = 1$ [25] obtained by combining in quadrature the Type A of Table 3 with the Type B uncertainties of Table 1.

Table 3: Viscosity η, Type A uncertainty $u_A(\eta)$, and combined uncertainty $u_C(\eta)$ as a function of temperature T and pressure p for $\{x\mathrm{CO_2} + (1-x)\mathrm{CH_4}\}$ with $x = 0.5174$.[c] The density ρ_{EOS} used to determine the viscosity from the resonance curve was calculated from the GERG-2008 EOS implemented in REFPROP 9.1 [13, 14]. At all values of T and p the mixture was in a single phase.

T /K	p /MPa	ρ_{EOS} /kg·m^{-3}	η /µPa·s	$u_A(\eta)$ / µPa·s	$u_C(\eta)$ / µPa·s
229.6	10.168	598.1	66.46	0.10	0.46
229.5	10.963	604.4	67.90	0.37	0.59
229.4	11.654	609.8	68.74	0.55	0.72
229.3	12.980	618.4	70.30	0.24	0.54
229.5	13.698	621.9	72.10	0.30	0.57
229.5	14.200	624.7	72.31	0.30	0.57
229.0	14.501	627.9	73.00	0.41	0.64
257.9	12.165	472.1	42.74	0.35	0.45
257.9	14.190	505.0	47.00	0.22	0.39
258.0	16.209	528.1	50.83	0.37	0.50
257.9	18.239	547.3	54.10	0.70	0.79
257.8	19.252	555.5	54.96	0.31	0.49
257.8	21.263	569.6	57.50	0.26	0.47
257.9	22.280	575.8	59.03	0.33	0.52
257.9	23.289	581.6	59.79	0.30	0.51
288.1	1.438	19.3	13.49	0.04	0.10
288.1	1.553	20.9	13.50	0.06	0.11
288.1	2.042	28.0	13.69	0.08	0.12
288.1	2.553	35.8	13.88	0.04	0.10

---

[c] Standard uncertainties u for temperature T, pressure p and mole fraction x are $u(T) = 0.005$ K, $u(p) = 0.004$ MPa, and $u(x) = 0.0001$

288.1	3.073	44.0	14.02	0.04	0.10
288.1	3.570	52.2	14.25	0.04	0.10
288.2	4.066	60.8	14.42	0.08	0.13
288.2	4.594	70.4	14.68	0.04	0.11
288.1	5.123	80.5	14.98	0.06	0.12
288.1	5.405	86.2	15.19	0.03	0.11
288.2	6.609	112.3	15.93	0.04	0.11
288.2	7.116	124.4	16.36	0.06	0.12
287.7	7.818	143.2	17.11	0.07	0.13
287.7	8.134	151.7	17.48	0.04	0.12
287.8	8.895	173.8	18.45	0.08	0.15
288.2	9.140	180.3	18.92	0.10	0.17
287.8	9.137	181.2	18.89	0.07	0.15
287.8	9.866	204.5	20.11	0.10	0.17
288.2	11.159	246.8	22.81	0.22	0.27
287.7	11.663	265.8	23.84	0.05	0.17
287.7	12.567	295.9	25.98	0.24	0.30
288.2	13.180	312.9	27.21	0.09	0.21
287.7	13.512	324.8	28.19	0.09	0.21
287.7	14.605	354.3	30.51	0.24	0.32
288.2	15.201	366.6	31.46	0.15	0.26
287.7	15.897	383.9	33.11	0.09	0.24
287.7	17.472	413.4	35.99	0.19	0.31
288.2	19.138	437.2	38.29	0.12	0.29
287.7	19.398	442.4	39.20	0.20	0.34
288.2	21.458	465.9	41.92	0.20	0.35
287.7	21.895	472.1	42.55	0.37	0.47
288.2	23.984	490.8	45.12	0.34	0.46
288.2	25.172	500.9	46.21	0.15	0.35
287.7	25.061	501.3	46.33	0.30	0.44
288.2	26.302	509.7	47.48	0.54	0.63
287.8	31.033	541.7	52.70	0.08	0.37
317.9	1.389	16.6	14.57	0.08	0.13
317.9	1.545	18.5	14.62	0.08	0.13
317.8	2.056	25.0	14.79	0.06	0.12
318.0	2.566	31.6	15.00	0.02	0.10
318.0	3.069	38.3	15.18	0.07	0.13
318.0	4.578	59.6	15.71	0.16	0.20
318.0	5.085	67.2	15.87	0.05	0.12
318.0	6.297	86.2	16.46	0.09	0.14
318.1	6.520	89.8	16.48	0.03	0.12
318.1	7.151	100.4	16.89	0.07	0.13
318.1	7.212	101.4	16.88	0.05	0.13
318.1	8.226	119.2	17.51	0.07	0.14
318.1	9.335	139.8	18.20	0.04	0.13
318.1	10.457	161.7	19.16	0.10	0.17
318.1	11.460	182.0	20.13	0.06	0.15

318.1	12.573	205.2	21.23	0.09	0.17
318.1	13.584	226.5	22.35	0.16	0.22
318.1	14.713	250.0	23.77	0.09	0.19
318.1	15.239	260.7	24.32	0.13	0.21
318.1	15.724	270.5	25.02	0.12	0.21
318.1	16.254	281.0	25.62	0.24	0.30
318.1	17.842	310.6	27.89	0.14	0.24
318.1	20.300	351.1	31.22	0.13	0.25
318.1	21.518	368.6	32.36	0.17	0.28
318.1	22.819	385.7	34.05	0.16	0.28
318.1	24.011	400.0	35.06	0.22	0.32
318.1	25.249	413.7	36.36	0.14	0.28
318.1	26.412	425.5	37.81	0.16	0.30
318.1	27.392	434.9	39.09	0.27	0.38
318.1	28.884	448.0	40.47	0.19	0.34
318.1	30.364	460.0	41.87	0.21	0.35
318.1	31.857	471.1	43.41	0.16	0.33
347.9	1.555	16.9	15.86	0.13	0.17
347.9	1.745	19.0	15.84	0.13	0.17
347.9	1.956	21.4	15.92	0.10	0.15
347.8	2.161	23.7	15.99	0.13	0.17
347.9	2.361	26.0	15.92	0.16	0.19
347.9	2.566	28.4	16.03	0.11	0.16
347.8	2.764	30.7	16.06	0.07	0.13
347.8	2.964	33.0	16.12	0.11	0.15
347.8	3.169	35.4	16.15	0.06	0.13
347.8	3.278	36.7	16.16	0.05	0.12
347.8	3.485	39.2	16.31	0.05	0.12
347.8	4.003	45.4	16.48	0.09	0.14
347.7	4.516	51.8	16.65	0.06	0.13
347.8	5.009	57.9	16.82	0.10	0.15
347.8	5.509	64.3	16.96	0.11	0.16
347.8	5.514	64.3	17.01	0.04	0.12
347.8	6.032	71.1	17.14	0.05	0.13
347.8	6.512	77.4	17.31	0.05	0.13
347.8	7.016	84.2	17.46	0.03	0.12
347.8	7.538	91.3	17.66	0.09	0.15
347.8	8.039	98.2	17.95	0.08	0.15
347.8	8.528	105.1	18.12	0.14	0.19
347.8	9.051	112.6	18.36	0.04	0.13
347.8	10.090	127.7	18.90	0.07	0.15
347.8	10.617	135.6	19.14	0.09	0.16
347.8	11.109	142.9	19.48	0.12	0.18
347.8	11.596	150.3	19.76	0.13	0.18
347.8	12.118	158.3	20.08	0.11	0.18
347.8	12.605	165.8	20.43	0.10	0.17
347.8	13.204	175.0	21.02	0.10	0.17

347.8	13.713	182.9	21.32	0.09	0.17
347.8	14.226	190.9	21.72	0.08	0.17
347.8	14.732	198.7	22.05	0.12	0.19
347.8	16.775	230.1	23.64	0.15	0.22
347.8	18.782	259.9	25.33	0.21	0.27
347.8	20.792	288.1	27.32	0.14	0.24

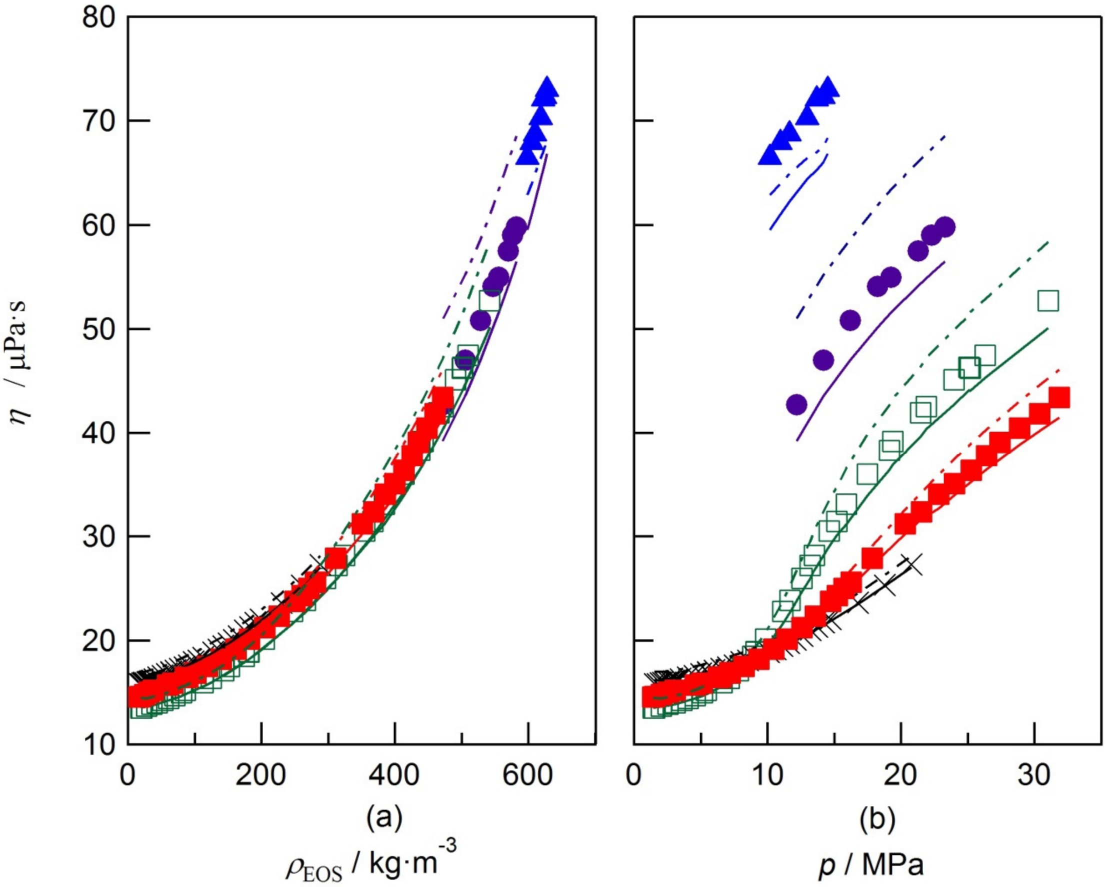

Figure 1. Measured viscosity, η, for $\{x\mathrm{CO_2} + (1+x)\mathrm{CH_4}\}$ with $x = 0.5174$ as a function of (a) mass density, ρ_{EOS}, and, (b) pressure, p. ▲, $T = 229$ K; ●, $T = 258$ K; □, $T = 288$ K; ■, $T = 318$ K; ×, $T = 348$ K. Viscosity estimated from the ECS model within REFPROP [13, 14] are shown as solid lines, ——; predictions obtained from SUPERTRAPP within MultiFlash [17] are shown as dash-dotted lines, — - .

The viscosities listed in Table 3 along five isotherms are shown in Figure 1 along with the viscosities predicted from both the ECS model in REFPROP [13, 14] and the SUPERTRAPP based model within MultiFlash. [17] The results deviate by a statistically significant margin of between -2 % at ($\rho < 20$ kg·m^{-3}), increasing to +11 % at $\rho > 600$ kg·m^{-3}. The consistent deviations at lower temperatures suggest the temperature dependence of the REFPROP ECS model may require adjustment. At lower temperatures and higher densities the predictions obtained from the ECS and SUPERTRAPP models differ by about 25 %, however, the viscosity measurements reported herein lie between the two models for all but the lowest temperature isotherm.

The fractional difference between the measured viscosity and the values estimated from the ECS model are shown as a function of mass density in Figure 2; it is clear the temperature dependence of the measured viscosity is lower than that predicted by the ECS model.

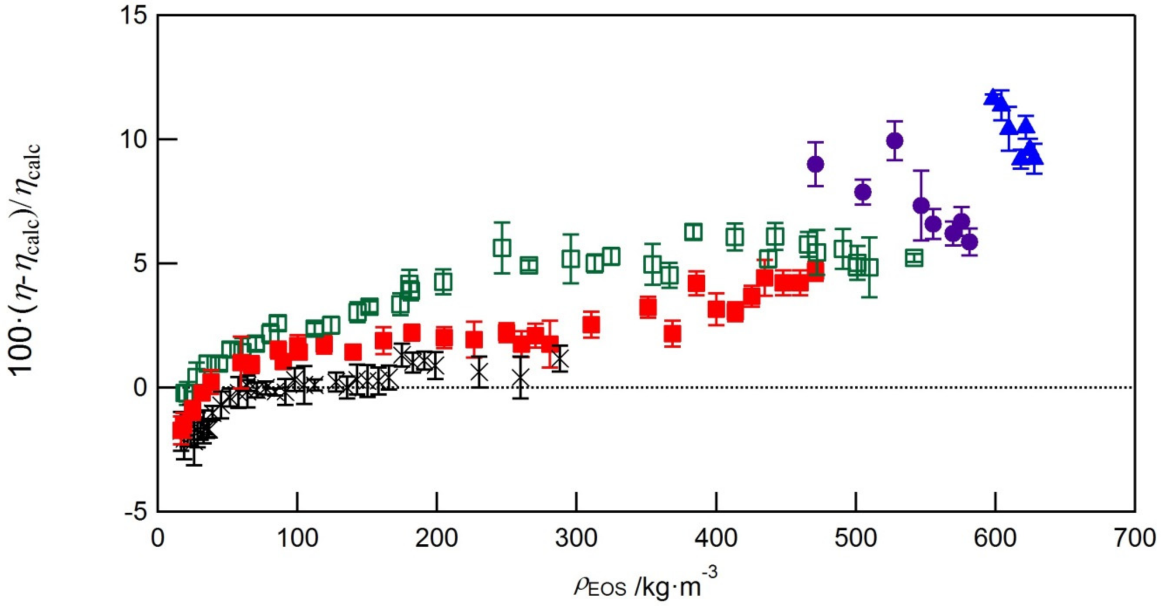

Figure 2. Fractional differences between the measured viscosity, η, and viscosity calculated, η_{calc}, using the REFPROP ECS model [13, 14] for $\{x\mathrm{CO_2} + (1+x)\mathrm{CH_4}\}$ with $x = 0.5174$ as a function of density, ρ_{EOS}. ▲, $T = 229$ K; ●, $T = 258$ K; □, $T = 288$ K; ■, $T = 318$ K; ×, $T = 348$ K. Vertical lines are Type A uncertainties.

The viscosities of $\{x\mathrm{CO_2} + (1\text{-}x)\mathrm{CH_4}\}$ reported by De Witt and Thodos [9] ($x = 0.536$) and Kestin et al. [10,11] ($x = 0.4357$) are compared in Figure 3, and are shown together with our results as relative differences from the estimates obtained using the ECS model in REFPROP. The results reported by Kestin et al. [10,11] measured with an oscillating disk viscometer (with a stated accuracy of ± 0.1 % at 25 °C), were at densities below 50 kg·m^{-3} while the results of De Witt and Thodos [9], obtained with a capillary viscometer (uncertainty not stated, but was fit to their correlation equation with a standard error of 3 % and a maximum deviation of 5 % relative), extended to densities up to 792 kg·m^{-3}. The variation of the deviations shown in Figure 3 for both these reported viscosities follows a pattern similar to that observed for our results.

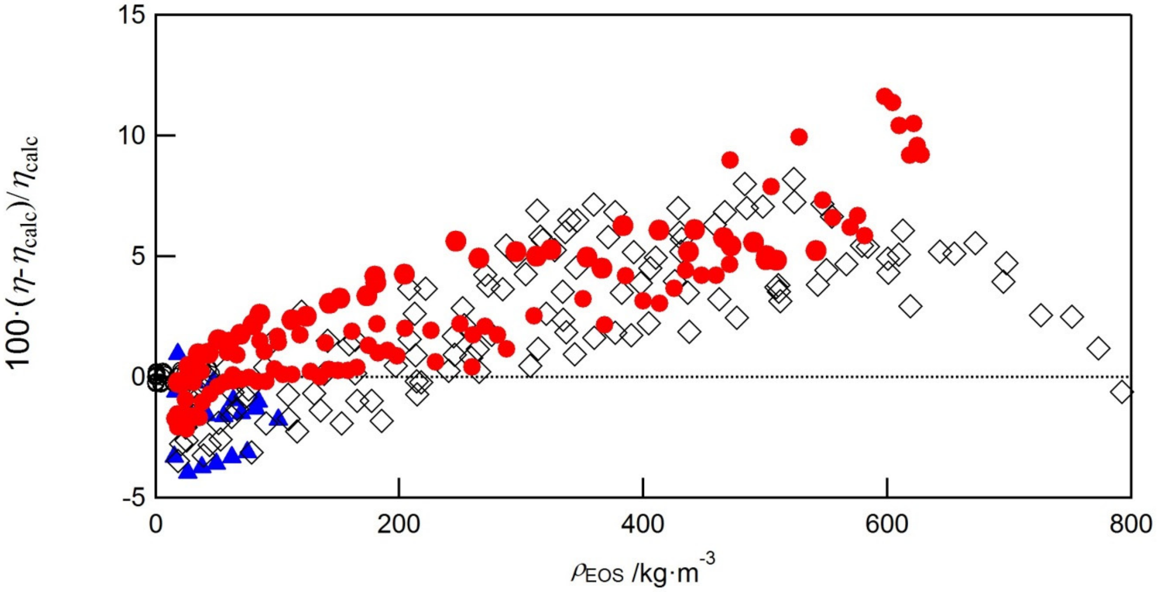

Figure 3. Fractional differences between the measured viscosities, η, and the viscosity calculated, η_{calc}, obtained from the ECS model in REFPROP for the $\{x\text{CO}_2 + (1+x)\text{CH}_4\}$ as a function of density, ρ_{EOS}. ●, this work x = 0.5174; ▲,Locke *et al.*,[8] x = 0.57; ○, Kestin et al. [10,11], x = 0.3257, 0.4806, 0.6624, 0.8565; and ◇, De Witt and Thodos [9], x = 0.245, 0.536, 0.757.

We have also compared our results with the predictive estimates of viscosity obtained from the LJ correlation based on molecular dynamic simulations, which does not contain any binary interaction parameters, and is specifically intended for acid-gas mixtures using a corresponding states scheme combined with a van der Waals one fluid approximation [20]. As Figure 4 shows, the relative deviations of these predictions, η_{MD} from the measured viscosities are between -3.5 % and +4.2 %, which is larger than the combined experimental relative uncertainty of 0.68 % but considerably less than the differences of the data from both the ECS model of REFPROP and the SUPERTRAPP model of MultiFlash.

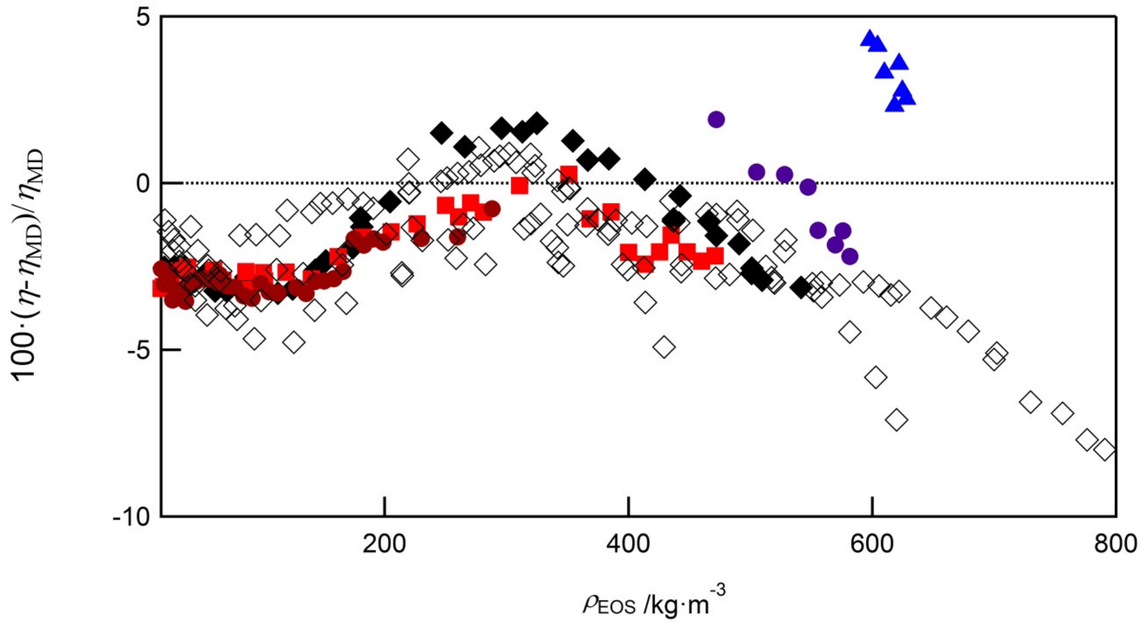

Figure 4. Fractional differences between the measured viscosity, η, and viscosity calculated, η_{MD}, using the molecular dynamic simulation models of Galliero *et al.* [20] for $\{x\text{CO}_2 + (1+x)\text{CH}_4\}$ with $x = 0.5174$ as a function of density, ρ_{EOS}. This work: ▲, $T = 229$ K; ●, $T = 258$ K; ◆, $T = 288$ K; ■, $T = 318$ K; ●, $T = 348$ K; ◇, De Witt and Thodos [9] with $x = 0.245, 0.536, 0.757$.

To understand these deviations, we recall here that this approach assumes that molecules can be modeled by spheres interacting according to a simple two parameter Lennard Jones potential. This is an imperfect representation of both methane and carbon dioxide [26-28] but nevertheless it achieves a better description of the mixture viscosity than either of the other corresponding states-type models. At low temperatures (solid triangles in Figure 4), the underestimation generated by the LJ correlation is related to the fact that the LJ model does not take into account the quadrupole moment of CO_2 [26]. At high temperatures, the LJ correlation generally overestimates viscosity. This is probably due to the limited ability of the repulsive term of the LJ potential to describe CH_4 [26-28] or CO_2 [27] sufficiently accurately. A possible improvement of this viscosity correlation when dealing with such fluids would be to base it on the more flexible Mie potential instead of the LJ one. This interaction potential has already proved its efficacy in improving models of thermophysical properties compared to the LJ potential [27] but, for the time being, a viscosity correlation does not exist for such a Mie fluid.

4. Conclusions

A doubly-clamped vibrating-wire viscometer operated in steady-state mode was used to measure the viscosity of a CO_2+CH_4 mixture at temperatures from (229 to 348) K and pressures in the range (1 to 32) MPa. The measured viscosities of this binary mixture show large deviations (up to +11%) from the ECS model in REFPROP, with the deviations becoming more positive as temperature decreases and density increases. These results validate measurements in the literature made at a similar composition, and also extend the results to lower temperatures. These new data may be used to aid the development of more accurate, wide-ranging viscosity models for the CO_2 + CH_4 mixture. In particular, the results validate recent models based on molecular dynamics simulations developed to predict the viscosities of acid-gas mixtures, which had a maximum relative deviation of 4.2 % from the data.

Funding Sources

This work was supported by the Australian Research Council's Linkage Program (LP130101018). E.F.M. acknowledges Chevron for their support of the research through the Gas Process Engineering endowment.

Acknowledgements

The authors thank Schlumberger for allowing ARHG to collaborate with them on this project.

[1] World Energy Outlook, International Energy Agency, http://www.worldenergyoutlook.org/media/weowebsite/2008-1994/weo2008.pdf, ISBN: 978-92-64-04560-6, 2008.
[2] A. Honari, T.J. Hughes, E.O. Fridjonsson, M.L. Johns, E.F. May, Int J Greenh Gas Con 19 (2013) 234-242.
[3] T.J. Hughes, A. Honari, B.F. Graham, A.S. Chauhan, M.L. Johns, E.F. May, Int J Greenh Gas Con 9 (2012) 457-468.
[4] J.L.V. Nichols, B.M. Friedman, A.L. Nold, S. McCutheon, A. Goethe, Processing technologies for CO2 rich gas, Proceedings of the 88th Annual Convention of the Gas Processors Association, San Antonio, TX 2009.
[5] T.J. Hughes, M.E. Kandil, B.F. Graham, E.F. May, Int J Greenh Gas Con 31 (2014) 121-127 10.1016/j.ijggc.2014.09.020.
[6] M.M. Weiss, A. Schriefl, Rectisol and oxyclaus: mature processes still going strong, 10th European Gasifaction Conference, Amsterdam, The Netherlands, 2010.
[7] V. Vesovic, Int J Thermo 22 (2001) 415-426.
[8] C.R. Locke, P.L. Stanwix, T.J. Hughes, A. Kisselev, A.R.H. Goodwin, K.N. Marsh, E.F. May, J Chem Eng Data 59 (2014) 1619-1628 10.1021/Je500083n.
[9] K.J. Dewitt, G. Thodos, Can J Chem Eng 44 (1966) 148-151.
[10] J. Kestin, J. Yata, J Chem Phys 49 (1968) 4780.
[11] J. Kestin, S.T. Ro, Berich Bunsen Gesell 78 (1974) 20-24.
[12] W.M. Jackson, The Journal of Physical Chemistry 60 (1956) 789-791.
[13] E. Davani, G. Falcone, C. Teodoriu, W.D. McCain Jr, J Nat Gas Sci Eng 12 (2013) 43-55.
[14] P.L. Stanwix, C.R. Locke, T.J. Hughes, M.L. Johns, A.R.H. Goodwin, K.N. Marsh, E.F. May, J Chem Eng Data (2014) 10.1021/je500857w.
[15] O. Kunz, R. Klimeck, W. Wagner, M. Jaeschke, The GERG-2004 Wide-Range Equation of State for Natural Gases and Other Mixtures, de Recherches Gazières, Groupe Européen. VDI Verlag, 2007.
[16] E.W. Lemmon, M.L. Huber, M.O. McLinden, NIST Standard Reference Database 23: Reference Fluid Thermodynamic and Transport Properties-REFPROP, Standard Reference Data Program, National Institute of Standards and Technology, Gaithersburg, VA, 2013.
[17] MultiFlash, InfoChem KBC Advanced Technologies PLC, 2014.
[18] User Guide for Models and Physical Properties, InfoChem/KBC Advanced Technologies PLC, 2014.
[19] G. Galliéro, C. Boned, A. Baylaucq, Ind Eng Chem Res 44 (2005) 6963-6972.
[20] G. Galliéro, C. Boned, A. Baylaucq, F. Montel, SPE Journal 15 (2010) 682-688.
[21] F. Ciotta, J.M. Trusler, J Chem Eng Data 55 (2009) 2195-2201.
[22] T. Retsina, S. Richardson, W. Wakeham, Appl Sci Res 43 (1986) 127-158.
[23] A.R.H. Goodwin, K.N. Marsh, J Chem & Eng Data 56 (2010) 167-170.
[24] C. Harrison, M. Sullivan, S. Godefroy, N. Matsumoto, A.R. Goodwin, K. Hsu, J Chem Eng Data 52 (2007) 774-782.
[25] B.N. Taylor, Guidelines for Evaluating and Expressing the Uncertainty of NIST Measurement Results (rev), DIANE Publishing, 2009.
[26] G. Galliéro, C. Nieto-Draghi, C. Boned, J.B. Avalos, A.D. Mackie, A. Baylaucq, F. Montel, Ind & Eng Chem Res 46 (2007) 5238-5244.
[27] C. Avendano, T. Lafitte, A. Galindo, C.S. Adjiman, G. Jackson, E.A. Müller, J Phys Chem B 115 (2011) 11154-11169.
[28] G. Galliéro, C. Boned, A. Baylaucq, F. Montel, Phys Rev E 73 (2006) 061201.